Effect of Thermodynamic Interactions on Reactions at Polymer/Polymer Interfaces

Todd D. Jones,[‡,§] Jonathan S. Schulze,[⊥,‡] Christopher W. Macosko,[*,‡] and Timothy P. Lodge[†,‡]

Department of Chemistry and Department of Chemical Engineering and Materials Science, University of Minnesota, Minneapolis, Minnesota 55455

Received April 15, 2003; Revised Manuscript Received July 30, 2003

ABSTRACT: We have examined the effect of monomer structure on amine−anhydride reactions at a polymer−polymer interface. The thermodynamic interaction parameter χ was varied by changing the backbone chemical structure, holding molecular weight constant. To eliminate the effects of mixing, experiments were performed with bilayer thin films of end-functional polymers. Using a combination of size exclusion chromatography with fluorescent labeling, we measured the extent of reaction of anhydride-terminal poly(methyl methacrylate) and polystyrene with amine-functional polystyrene, polybutadiene, poly(ethylene/ethylethylene), and poly(dimethylsiloxane). Interfacial structure was observed by atomic force microscopy. Both the conversion to block copolymer and the degree of interfacial roughening are suppressed with increasing χ. This suppression may be related to reduced solubility of the reactive homopolymers in the formed block copolymer and to decreased interfacial volume for reactions to occur. Viscosity does not play a significant role in these studies. In melt blends of similar polymers prepared in a cup-and-rotor mixer, the rate of reaction and extent of conversion also generally decrease with increasing χ. The rates are up to 100 times faster, suggesting that convection sweeps away block copolymer that forms at the interface. These results indicate that thermodynamic interactions play a significant role in determining rates of reaction at polymer interfaces.

Introduction

Reactive compatibilization has been widely used as a means of controlling the morphology and material properties of immiscible polymer blends. Many polymers have been examined in these reactive blends, primarily through changes in blend morphology in the presence of reaction.[1−3] While morphology development during mixing of nonreactive polymers has been studied extensively,[4−6] reactive blends are more complex. Consequently, additional parameters are significant, in particular those that affect rates of copolymer formation and thus blend morphology. Recent studies have also shown that very rapid coupling reactions between polymers can result in high amounts of block copolymer, suggesting a solvent-free melt method for their production.[7−12]

Our strategy has been to simplify reactive blending studies by using end-functional, monodisperse materials to form diblock copolymer at the interface between two immiscible phases.[13,14] Further understanding is achieved by separating the effect of mixing from that of reaction, using bilayer samples. Under these conditions, interfacial roughening has been observed in a variety of systems, including PMMA-anh/PS-NH_2,[15−18] nylon/polysulfone,[19] and PS/poly(styrene-*r*-maleic anhydride).[20,21] Schulze et al. found that the extent of reaction and interfacial roughening increased with lower matrix molecular weight and with higher reactant concentration.[16,17,37] Yin et al. also observed that extent of reaction and roughening increased with lower molecular weight functional polymers.[18] However, each of these reports has relied on a single polymer system, and no attempt has been made to compare polymers with similar reactive group chemistry but different monomer units.

Our goal is to examine the effect of monomer structure, and thus thermodynamic interactions, on reactions at immiscible polymer/polymer interfaces. Recently we developed a synthesis method for fluorescently labeled reactive polymers, enabling the measurement of small quantities of copolymer formation using size exclusion chromatography (SEC). This SEC/fluorescence technique was demonstrated on dilute polymer blends containing 1% or less of reactive components[22] and found to be in good agreement with conversion measurements by forward recoil spectroscopy on layered polymer films.[23] We have used this technique, in combination with AFM, to examine reactions between a variety of polymers. We have synthesized four different amine-terminal polymers of about the same molecular weight and reacted them with three anhydride-terminal polymers labeled with anthracene. These combinations give χ values ranging from 0.02 to 0.3. We have compared these quiescent reactions to reactive coupling during melt mixing of similar polymers.

Experimental Section

Materials. Silicon wafers approximately 0.5 mm thick were broken into 3 cm × 3 cm squares. Cyclohexane, dichloromethane, methanol, hexanes, tetrahydrofuran (THF), and toluene (Aldrich) were dried prior to use where necessary by standard techniques. Phenyl isocyanate (Aldrich) and Irganox 1010 (Ciba-Geigy) were used as received. Polybutadiene-amine (PB-NH_2) and poly(ethylene/ethylethylene)90-amine (PEE-NH_2), anthracene-labeled polystyrene-anhydride (*PS-anh), anthracene-labeled PMMA-anh (*PMMA-anh), polystyrene-anhydride (PS-anh), and poly(methyl methacrylate)-anhydride (PMMA-anh) were synthesized as described elsewhere.[22,24,25]

† Department of Chemistry.
‡ Department of Chemical Engineering and Materials Science.
§ Present address: 3M Science Research Center, 3M Company, Saint Paul, MN 55144-1000.
⊥ Present address: ExxonMobil Chemical Company, Baytown, TX 77520-2101.
* Corresponding author.

10.1021/ma0344846 CCC: $25.00
Published on Web 08/29/2003

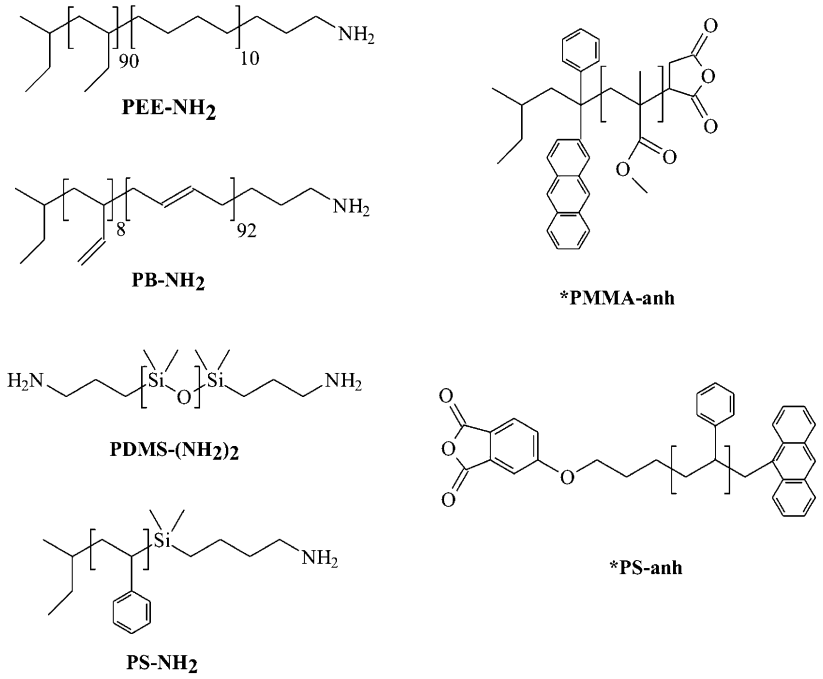

Figure 1. Chemical structure of polymers used in interfacial coupling studies.

Table 1. Reactive Polymer Characteristics

polymer	M_n (g/mol)	M_w/M_n	f^c	η_0, 175 °C (Pa s)
anhydride[a]				
*PMMA-31-anh	31 200	1.03	0.95	600000
*PMMA-12-anh	11 800	1.12	0.95	7000[b]
*PS-53-anh	53 000	1.09	0.72	1700
amine				
PS-NH_2	18 000	1.1	0.90	28
PEE-NH_2	18 000	1.05	0.70	2.2
PB-NH_2	25 000	1.10	0.83	14
PDMS-$(NH_2)_2$	22 000	1.43	1.65	0.27

[a] An asterisk in the polymer name indicates the presence of a fluorescent label. [b] Viscosity is estimated from literature values as the quantity of polymer was insufficient to measure directly. [c] End functionality determined by solution coupling with PEG.[26]

An asterisk will be used to identify fluorescently labeled polymers in this paper. Polystyrene-amine (PS-NH_2) was synthesized by J. Cernohous, as described in the literature.[26] Difunctional poly(dimethylsiloxane)-amine (PDMS-$(NH_2)_2$) was obtained from Gelest, Inc. Difunctional poly(dimethylsiloxane)-anhydride (PDMS-$(anh)_2$) was synthesized by M. Maric.[27] All polymers were characterized by ^{1}H NMR spectroscopy and PEG solution coupling to determine functionality.[26] Polymer chemical structures are shown in Figure 1. With the exception of the PDMS-$(NH_2)_2$, the polymers were of high functionality and nearly monodisperse, as preferred for successful SEC measurements of conversion.[13] Polymer properties, including viscosity as measured on a Rheometrics DSR controlled stress rheometer using 25 mm parallel plates under a nitrogen purge, are summarized in Table 1. As seen in this table, the polymers cover a wide range in viscosity. The reacted pairs are listed in Table 2.

Sample Preparation: Spin-Coating and Annealing. Samples of the fluorescent polymer, either *PMMA-anh or *PS-anh (0.1−0.25 g), were dissolved in toluene (5 mL). The solutions were spun onto a 3 cm by 3 cm square piece of silicon at room temperature and 1800 rpm for 35 s to obtain a flat film. The film thickness was measured by ellipsometry and ranged from 90 to 300 nm depending on solution concentration and molecular weight of the polymer. Subsequently, amine-functional polymers were either solvent cast from cyclohexane (PS, PB, PEE) onto *PMMA-anh or spun-coat from hexanes (PB, PEE) onto *PS-anh, yielding a ≥ 1 μm thick film. Typical concentrations were 0.08 g of polymer in 2 mL of dry solvent, with 0.0040 g of Irganox 1010 as a thermal stabilizer. The resulting squares were broken into multiple pieces and placed in a custom-built vacuum oven. When amine-functional PDMS was the top layer, it was added directly to the *PMMA-anh or *PS-anh surface prior to annealing without spinning, due to its low viscosity. Sufficient PDMS was put on to completely wet the surface of the wafer. A piece of microscope coverslip glass was placed on top of each sample to provide a barrier to oxygen diffusion. This barrier prevented cross-linking of polybutadiene during annealing, which could lead to errors in analysis. The layered samples were annealed at 175 °C and 25 mTorr of vacuum, with samples removed at intervals ranging from 0.25 to 16 h. The bilayer films were quenched on dry ice and stored at −15 °C in the dark after annealing.

SEC Measurements of Conversion. The annealed samples were dissolved in THF (2 mL) containing 1% of phenyl isocyanate. This reagent reacts with unconverted polymeric amine to prevent coupling in solution. The solution was then injected on a Waters 150C SEC at 30 °C with THF as the mobile phase. A series of three Phenogel 7.5 mm columns with pore sizes of 5×10^4, 5×10^3, and 5×10^2 Å were used. The resulting chromatograms were measured by a sequential series of a Hitachi fluorescent detector with an excitation wavelength of 358 nm and an emission wavelength of 402 nm, a UV detector set at a wavelength of 254 nm, and a differential refractomer.[22] The resulting chromatogram was then fit to a series of Gaussian peaks to determine conversion.

Melt Blending. Melt blending was carried out in a Mini-MAX mixer at 200 °C under a nitrogen purge, with three steel balls to improve mixing flow.[28] The total mass of each polymer blend was approximately 300 mg. Samples (∼10 mg) were taken periodically up to 20 min to obtain an estimate of conversion vs time and quenched in water. The samples were then dissolved in THF with phenyl isocyanate to quench the remaining reactive groups, and conversion was analyzed by SEC as described above.

Atomic Force Microscopy (AFM). Samples for atomic force microscopy were prepared by placing the entire sample in a selective solvent overnight at room temperature, thereby dissolving away the top thin film layer. This process also separated the top glass coverslip from the layered sample. PB, PEE, and PDMS were removed by dissolving in hexanes. PS was removed by dissolving in an 87:13 vol:vol mixture of cyclohexane and toluene to completely remove the polystyrene layer without disturbing the underlying PMMA. Surface

Table 2. Structure of Annealed Thin Films at 175 °C after 4 h

polymer 1	polymer 2	η_r	t (nm)	Σ (4 h) (chain/nm^2)	χ (175 °C)	a_I (nm)	roughness (nm, rms)
*PMMA-31-anh	PS-NH_2	4.7×10^{-5}	230, 210	0.78	0.017[b]	4.2	42
	PB-NH_2	2.3×10^{-5}	230, 210	0.42	0.085[d]	1.8	38
	PEE-NH_2	3.7×10^{-6}	230, 210	0.33[a]	0.11[d]	1.3	12
	PDMS-$(NH_2)_2$	4.5×10^{-7}	130	0.32[a]	0.32[d]	0.7	0.62
*PMMA-12-anh	PS-NH_2	0.0040	120	1.9	0.017[b]	4.7	
	PB-NH_2	0.0020	150	1.1	0.085[d]	1.8	
	PEE-NH_2	0.00031	120	0.87	0.11[d]	1.4	
	PDMS-$(NH_2)_2$	3.9×10^{-5}	120	0.87	0.32[d]	0.7	
*PS-53-anh	PEE-NH_2	0.0013	90	0.16	0.038[b]	2.4	14
	PDMS-$(NH_2)_2$	0.00016	90	0.17[a]	0.19[c]	0.9	1.2

[a] Data estimated by interpolation from surrounding data points. [b] Values of χ as reported by Balsara.[39] [c] Value of χ reported by Shefelbine et al.[40] [d] Values of χ based on extrapolation of known χ for blends to unmeasured blends $\chi_{31} = (\chi_{32}^{1/2} + \chi_{21}^{1/2})^2$. A reference volume of 100 Å^3 is assumed.

structure was examined using a Digital Instruments Nanoscope III AFM with a pyramidal Si_3N_4 tip in contact mode, over a 2 μm × 2 μm area at a scan rate of 2 Hz and angle of 90°. Images were taken at three different locations, with the root-mean-square (rms) roughness measured in each position. These results were averaged to obtain the reported rms roughness. We examined the surface of *PS-anh and *PMMA-anh films before and after solvent casting and observed no significant surface roughening. We also annealed the films in the presence of a nonfunctional top layer for 3 h and did not observe distortion of the surface after its removal under the same conditions.

Results

We analyze our results in terms of interfacial conversion Σ, the number of copolymer chains per unit area. To determine Σ, both the film thickness and the conversion of labeled polymer are required. Film thicknesses for the lower layer and the estimated value of χ for each pair are summarized in Table 2. The thickness of the upper layer was much greater than the lower layer. This was verified by the absence of color in the films, indicating thickness greater than 1 μm. By having a thick upper film, we provided a large reservoir of functional polymer, so that the lower film would always be the limiting reagent.

After dissolving all polymer present and running SEC measurements, we can determine the fraction of fluorescent chains converted to block copolymer. Knowing the thickness of the lower fluorescent film t, the density of the polymer in the melt at the annealing temperature ρ, the molecular weight M_n, and the measured degree of conversion x, we can calculate the interfacial conversion Σ as follows:

$$\Sigma = \frac{xt\rho}{M_n} N_A \qquad (1)$$

where N_A is Avogadro's number and we have assumed the presence of a flat interface. By couching the data in terms of Σ, rather than overall conversion, we are able to directly compare experiments with different film thicknesses. Measurements on anhydride-functional polymers annealed in the absence of any complementary functional groups showed that some coupling occurred between the labeled chains. This side reaction may involve the anthracene groups, which are not completely inert to reaction with each other.[30] We corrected for this by annealing bare films in the presence of nonfunctional complementary polymer under similar conditions and subtracting the measured conversion for self-coupling (typically ~10% of the total conversion) from the measured bilayer conversion to obtain the extent of reaction between complementary chains. This results in an uncertainty in all measurements of Σ of approximately ±0.1 chains/nm^2. Our results for the functional polymer samples are summarized in the following sections.

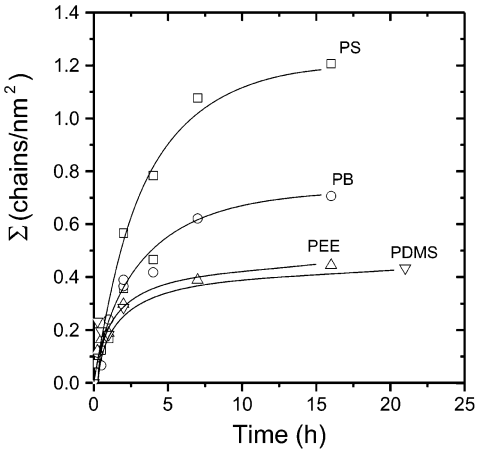

Figure 2. Interfacial conversion vs time for reactive films of *PMMA-31-anh with complementary functional polymers annealed at 175 °C. PS-NH_2 (□) is the most reactive, followed by PB-NH_2 (○), PEE-NH_2 (△), and PDMS-$(NH_2)_2$ (▽). The curves in all figures are drawn as a guide to the eye.

Fluorescent PMMA Layered Samples. We observed significant formation of block copolymer at the *PMMA-31-anh−polymer interface for all polymer pairs. The interfacial conversion of block copolymer, Σ, as a function of time is shown in Figure 2. From the lamellar spacing of pure diblock copolymers of similar molecular weight[29] the interface should become saturated at about 0.2 chains/nm^2. All the pairs reach saturation in about 2 h. Within the accuracy of our data all the pairs have the same reaction rate in this short time region. However, at longer times there are significant differences, and the reaction appears to slow dramatically or stop after 10−15 h. PS showed the highest level of coupling, followed by PB, PEE, and PDMS. There is no difference between PEE and PDMS within the experimental uncertainty. The maximum interfacial conversion with PS represents 29% conversion of the thinner PMMA layer while for PEE only 11% of the PMMA layer has reacted after 15 h.

We compare these results with the structure of the interface after 4 h of annealing. Figure 3 shows images of the *PMMA-31-anh interface obtained by AFM. Significant roughening of the surface is observed for all of the samples, with the exception of the case where PDMS was the upper film. This roughening can be quantified in terms of root-mean-square roughness, a

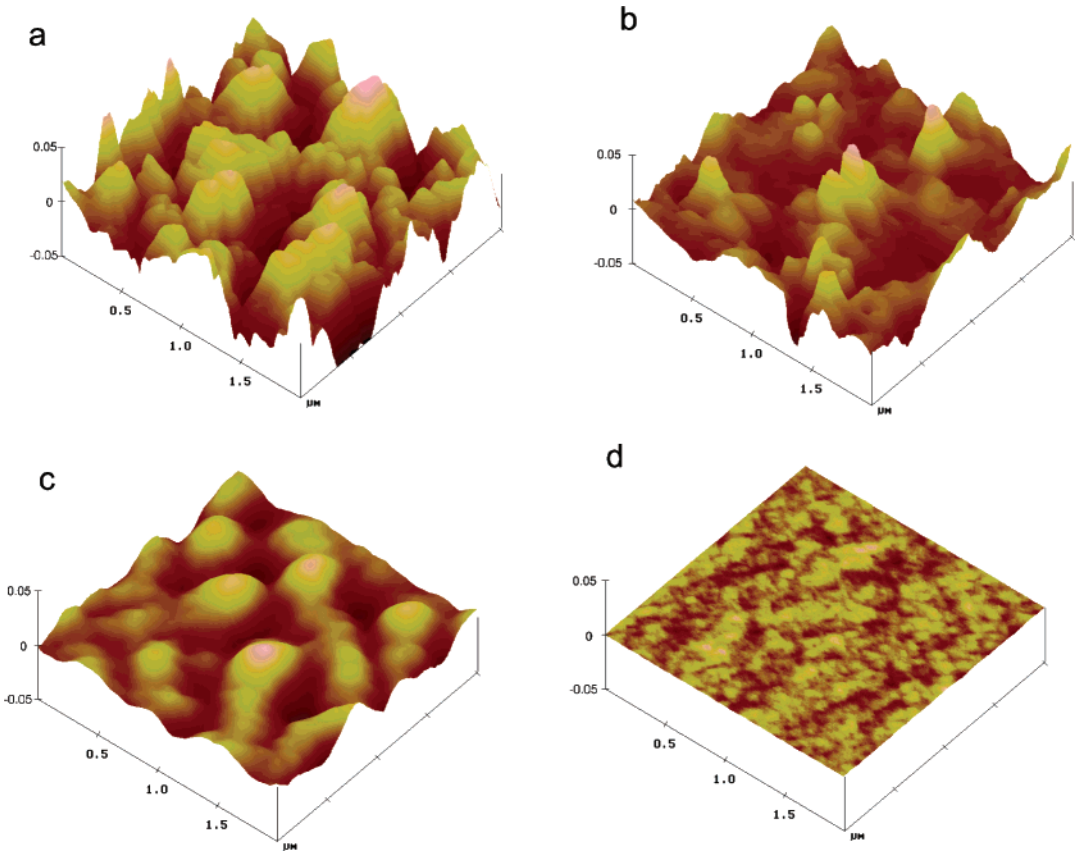

Figure 3. AFM images of interfacial structure of *PMMA-31-anh thin films after 4 h of annealing. Horizontal dimensions in all images are 2 μm by 2 μm, while vertical dimensions are 100 nm. The upper layer of polymer in each case has been removed by dissolving in selective solvent. The upper layers were (a) PS-NH_2, (b) PB-NH_2, (c) PEE-NH_2, and (d) PDMS-$(NH_2)_2$.

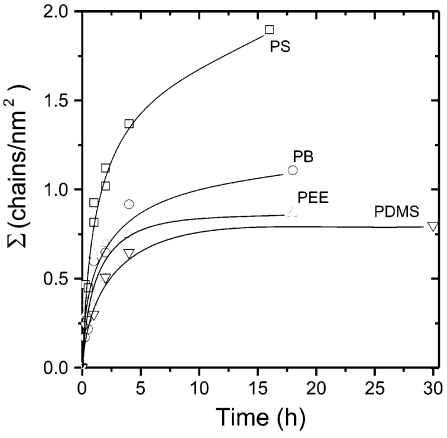

Figure 4. Interfacial conversion vs time for reactive films of *PMMA-12-anh with complementary functional polymers. The order of reactivity is the same as Figure 2, but the extent of conversion is increased. Upper layers were PS-NH_2 (□), PB-NH_2 (○), PEE-NH_2 (△), and PDMS-$(NH_2)_2$ (▽).

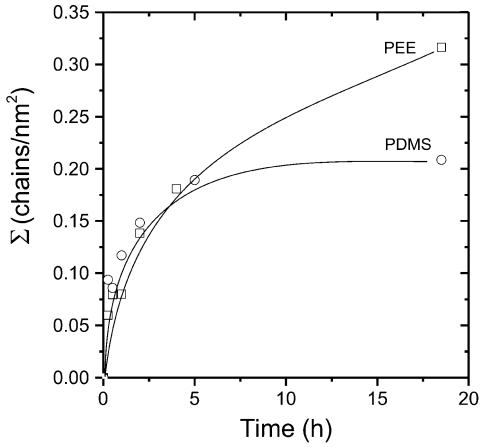

Figure 5. Interfacial conversion vs time for thin layer samples of *PS-53-anh with PEE-NH_2 (□) and PDMS-$(NH_2)_2$ (○).

measure of the deviation from the average height of the surface. These values are tabulated in Table 2. The extent of roughening increases with Σ except for PDMS. Note that the vertical scale in these images exaggerates the extent of roughening, and the minimum curvatures observed are >30 nm, the radius of the AFM tip. Increases in interfacial area due to roughening are no more than 20% and are thus insufficient to account for the large differences in Σ. Reduction of the molecular weight of the *PMMA-anh leads to higher levels of Σ. The interfacial conversion is shown as a function of time for bilayer samples containing *PMMA-12-anh in Figure 4. For all pairs of functional polymers, the interfacial conversion is consistently lower for *PMMA-31-anh than for *PMMA-12-anh. However, the polymer pairs follow the same order in terms of maximum interfacial conversion. Moreover, for PB, PEE, and PDMS the reaction appears to stop after 15 h or about 15% conversion of the PMMA layer. We were not able to obtain reliable AFM images of the *PMMA-12-anh surfaces. The low molecular weight may have made it more fragile and more susceptible to the solvents used to wash off the upper layers.

Fluorescent PS-anh Layered Samples. Slightly different results are obtained for *PS-anh thin film experiments as compared to *PMMA-anh. As shown in Figure 5, the interfacial conversion with PEE and

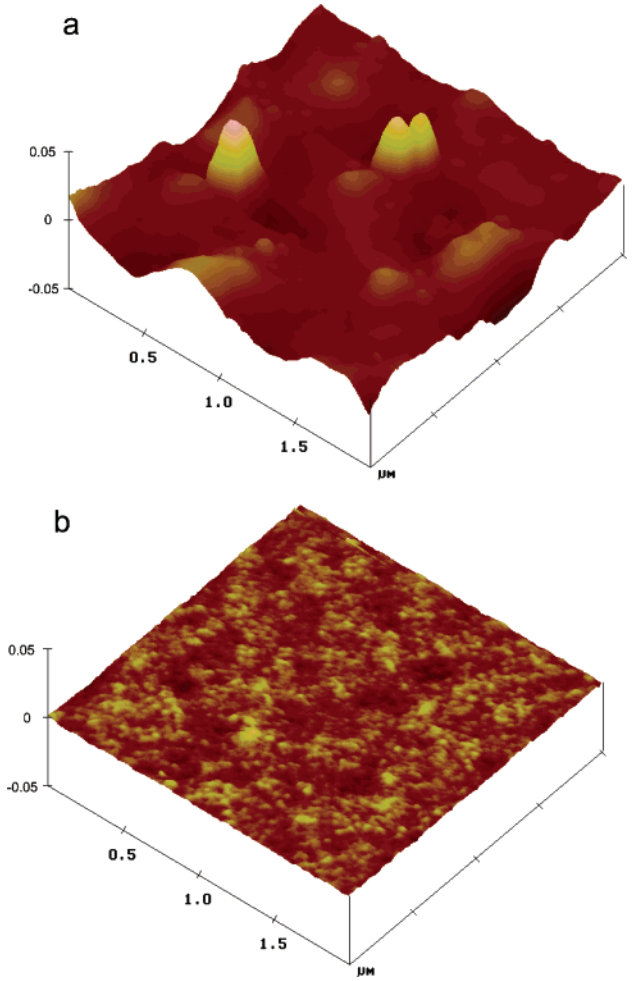

Figure 6. Interfacial structure of thin film samples containing *PS-53-anh after 4 h annealing at 175 °C. While the reactivities of the PEE-NH_2 (a) and PDMS-$(NH_2)_2$ (b) are similar, as shown in Figure 5, the interfacial structures are quite different.

PDMS is approximately the same after 4 h of annealing. However, after 4 h annealing time the interfacial topology of the two samples is significantly different. As with the *PMMA-anh, no interfacial roughening is observed for PDMS-$(NH_2)_2$ (Figure 6b). In contrast, the surface roughening for the PS−PEE pair is strong, as shown in Figure 6a. Figure 5 indicates that additional reaction occurred between the PS−PEE pair with longer annealing times, while Σ for PS−PDMS remains constant. However, there is only a single data point at longer times.

Discussion

In these experiments, we have observed two principal effects: an increase in the rate of reaction and the extent of reaction at long times with decreasing χ and an increase in interfacial roughening with decreasing χ. Our extents of conversion are measured in terms of Σ, the interfacial conversion. Except for the PS/PDMS pair, the maximum interfacial conversion values significantly exceed interfacial saturation coverage, $\Sigma^* \sim 0.2$ chain/nm^2. As mentioned above, the increase in area alone due to interfacial roughening cannot explain these high values. Lyu et al.[15] measured similar roughening with AFM for the interfacial reaction between PS-NH_2 and PMMA-anh but also observed by TEM that a lamellar block copolymer phase formed near the interface. This phase roughened and thickened to several hundred nanometers with time. Yin et al.[18] also observed roughening and a block copolymer phase at the interface of similar molecular weight PS-NH_2 and PMMA-anh; however, their phase appeared to be a disordered microemulsion. Our SEC method measures the total amount of block copolymer. Thus, the Σ values in Table 2 represent the total amount of block copolymer per unit cross-sectional area found in the bilayer samples.

The trend of increased rate and extent of reaction in these experiments with decrease in χ can be analyzed in terms of the interfacial volume available for reaction. Reaction between the bilayers should occur within the region where the chains overlap. The average interfacial width is related to the thermodynamic interactions and can be estimated from the relation derived by Helfand and Tagami[31]

$$a_{I\infty} = 2\left(\frac{b_1^2 + b_2^2}{12\chi}\right)^{1/2} \tag{2}$$

where b is the statistical segment length.[32] Broseta et al.[33] have developed a correction to this theory for finite molecular weight polymers.

$$a_I = a_{I\infty}\left[1 + \ln 2\left(\frac{1}{N_1\chi} + \frac{1}{N_2\chi}\right)\right] \tag{3}$$

where N_i is the number of statistical segments in polymer chain i. On the basis of these equations, we have calculated the interfacial widths reported in Tables 2 and 3. We observe that the maximum conversion increases with increasing interfacial width, as shown in Figure 7. In effect, a wider interface allows greater opportunity for complementary chains to react, enabling faster reactions and greater interfacial conversion. When interfacial conversion exceeds the saturation coverage, $\Sigma > \Sigma^*$, block copolymer must be leaving the initial interface. The rate of removal and the rate of reactive polymer penetration into the phase or emulsion that forms near the interface should both be governed by χ.

Interfacial width should also increase as block copolymer forms. However, Russell et al. demonstrated that the interfacial width between homopolymer PS and PMMA only increases by approximately 50% when PS−PMMA diblocks are present.[34] Similar effects might be expected with other polymer pairs and should also depend on χ.

A more significant effect of block copolymer formation may be its reduction of the interfacial tension. Lyu et al.[15] have argued that reduced interfacial tension will reduce energetic penalties for interfacial fluctuations, allowing for increased interfacial area. This will subsequently lead to increased formation of block copolymer. Machuga et al.,[35] in their studies of reactions between isocyanates and amine-functional polyol, argued that interfacial tension may, in fact, disappear. Jiao et al.[21] also argue for zero interfacial tension when $\Sigma \sim \Sigma^*$. Σ^* decreases with χ but only $\sim\chi^{1/6}$. If only interfacial tension governs interfacial reaction and it becomes zero at Σ^*, then, since for all the pairs in Figures 2 and 4 $\Sigma > \Sigma^*$, we would expect complete conversion for all the pairs. This is not observed.

Effect of Molecular Weight. Molecular weight plays an important role in polymer properties, including diffusivity and viscosity. One might initially expect the

Table 3. Characteristics of Melt-Mixed Blends

polymer 1	polymer 2	ϕ_1	χ (200 °C)	a_I (nm)	conversion[a] (20 min)
PMMA-anh (22 kg/mol)	PS-NH_2 (15 kg/mol)	0.62	0.017	4.2	0.92
PS-NH_2 (21 kg/mol)	PB-anh (25 kg/mol)	0.70	0.024	3.6	0.98
PS-anh (35 kg/mol)	PEE-NH_2 (18 kg/mol)	0.70	0.036	2.4	0.79
PEE-NH_2 (18 kg/mol)	PDMS-anh (28 kg/mol)	0.70	0.055	1.9	0.64[b]
PS-NH_2 (15 kg/mol)	PDMS-anh (28 kg/mol)	0.80	0.18	1.0	0.32

[a] Conversion of limiting polymer, based on available functionality. [b] 15 min.

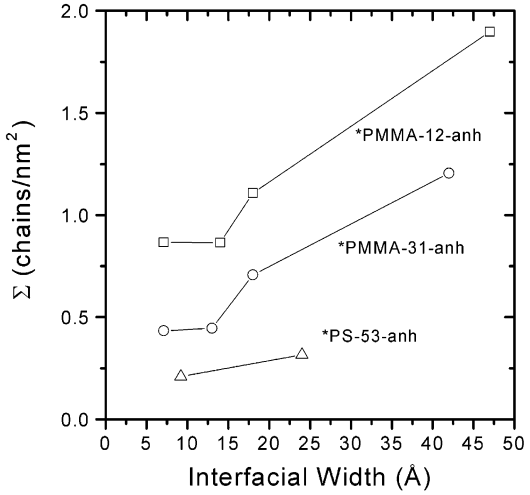

Figure 7. Maximum interfacial conversion Σ as a function of initial interfacial width. Data points include thin films containing (□) *PMMA-12-anh, (○) *PMMA-31-anh, and (△) *PS-53-anh. Interfacial widths are estimated from eq 3 using literature values of statistical segment length[32] and χ[39,40] and a reference volume of 100 Å^3. Two trends are evident from these results: as the interfacial width increases (and χ decreases), the maximum interfacial conversion also increases. Also, maximum conversion decreases with increasing molecular weight of the reactive component.

reaction rate, and extent of reaction, to be strongly dependent on the diffusivity. On the basis of literature reports for PS and PMMA,[36] we calculate that *PS-53-anh at 175 °C should have a diffusivity of $\sim 3 \times 10^{-12}$ cm^2/s, while *PMMA-31-anh and *PMMA-12-anh have diffusivities of $\sim 2 \times 10^{-14}$ and 1×10^{-13} cm^2/s, respectively. On this basis, functional PS should be more available for reaction, leading to higher interfacial conversion. Figure 7 indicates just the opposite. A similar case holds for the effects of viscosity on interfacial roughening. Jiao et al. have proposed that the more viscous phase controls the kinetics of interfacial roughening in a bilayer system.[21] However, it should be pointed out Jiao et al. annealed their samples only slightly above the T_g of one of the layers. Our results indicate that viscosity does not control interfacial conversion. In Figure 3 *PMMA-31-anh is the much more viscous component (see Table 1), but roughening ranges from significant to nonexistent. PS-anh has a viscosity 350 times less than that of PMMA, but as Figure 7 shows, it has the lowest extent of reaction. Given that there is little driving force for flow present in a quiescent bilayer system of this type, viscosity is less important. Whereas Machuga et al. argued that a concentration gradient drives very rapid roughening,[35] we do not observe reaction occurring at the high rates seen in their much lower molecular weight system. Similarly, diffusion of the base homopolymer does not seem to control the structure. Thus, interfacial conversion does not scale with either viscosity or diffusion coefficient.

While viscosity and the diffusion coefficient are not critical, molecular weight of the polymers does appear to play a significant role. As shown in Figure 7, the maximum interfacial conversion decreases with increasing molecular weight at a given interfacial width. This is in agreement with observations by Schulze et al.[16,17,37] and Yin et al.,[18] who found decreasing conversion and interfacial roughening for PS/PMMA thin film bilayer samples with increasing matrix molecular weight. Yin et al. argue that interfacial conversion should correlate with χN, the driving force for phase separation. This appears valid for the PS/PMMA results but not when χ is large. For example, χN for PDMS and *PMMA-12-anh is much higher than χN for PEE or PB with *PMMA-31-anh, yet the latter show significantly lower conversion. It is likely that a decreased concentration of functional groups, which scales with $1/M_n$, limits the chains' ability to meet and react. In addition, high molecular weight block copolymers may suppress interfacial fluctuations. Block copolymer asymmetry may also be important. In our study diblocks formed from *PS-53-anh are the most asymmetric and show the lowest conversion. Molecular weight thus plays a critical role in determining extents of reaction and roughness in these thin bilayer samples.

A puzzling result is the lack of roughness in the PDMS/PMMA and PDMS/PS interfaces (Figures 3 and 6) given that the interfacial conversions are similar to the interfaces with PEE which do show roughness. The PDMS pairs have the highest χ values and thus possibly higher interfacial tension. Reactively formed diblocks may be able to leave the interface without it roughening or undulations flatten out.

Melt Blending of End-Functional Polymers. We can also compare our bilayer film results with rates of reaction observed for similar polymers in bulk mixing. The polymers we have examined include PS and PB,[7,24] PS and PMMA,[7] PS and PEE,[24] PS and PDMS,[27] and PEE and PDMS.[24] Several of these polymers do not appear in Table 1; their synthesis is described in refs 7, 10, and 18. Characteristics of these blends are summarized in Table 3, and conversion vs mixing time is shown in Figure 8.

In this figure we see that, as with the bilayer films, reaction rate increases with interfacial width or decreasing χ; however, it is nearly 100 times faster and conversion is significantly higher. The same argument that decreasing χ increases the interfacial volume available for reaction and reduces the interfacial tension should apply to these bulk mixed samples. The remarkable increase in reaction rate has also been observed by Schulze et al.[16,17,37] and Lyu et al.[15] We attribute the dramatic increase in rate and conversion to convection of block copolymer away from the interface. In the bilayer films the block copolymer phase at the interface presents a considerable barrier to diffusion;[38] moreover, it thickens with time, effectively shutting off the reaction before the lower film can be consumed. Pairs with

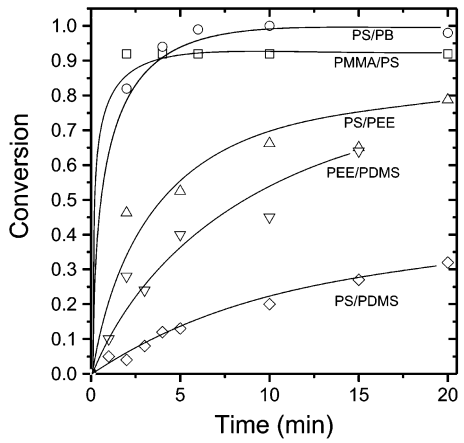

Figure 8. Conversion vs time for melt-mixed blends of two polymers with terminal functionality. Blends include 70% PS-NH_2/30% PB-anh (○), 62% PS-NH_2/38% PMMA-anh (□), 70% PS-anh/30% PEE-NH_2 (△), 70% PEE-NH_2/30% PDMS-$(anh)_2$ (▽), and 80% PS-NH_2/20% PDMS-$(anh)_2$ (◇). Conversion is calculated on the basis of the amount of the reactive minor component. Rates of reaction generally increase with interfacial width (see Table 3).

high χ will be less soluble in the block copolymer, which will further limit diffusion and may explain their relatively lower conversion.

Conclusions

The effect of monomer structure on reactions in heterogeneous melt blends between end-functional polymers has not previously been extensively examined. By changing the chemical nature of the polymer backbone, we change the interaction parameter χ, which subsequently alters both the interface width and the interfacial tension. We have studied this effect in both bilayer thin films and in melt blends. Using fluorescently labeled polymers and size exclusion chromatography, we have observed the amount of block copolymer formed in reactions of anhydride-functional PMMA and PS with amine-functional PS, PB, PEE, and PDMS in layered samples. Increasing the segregation strength of the two polymers decreases the maximum amount of block copolymer formed and suppresses interfacial roughening. Increasing the molecular weight similarly leads to decreases in interfacial roughening and maximum conversion, presumably through lower concentration of functional groups.

We observe a similar effect of interaction parameter in heterogeneous melt blends of end-functional polymers prepared in a MiniMAX melt mixer. While we are unable to completely decouple viscosity and segregation strength in melt blending, we observe that, like the bilayer film results, reaction rates and amounts of block copolymer formed decrease with increasing χ. However, with melt mixing, reaction rates and conversion are much higher due to convection sweeping away block copolymer as it forms at the interface.

The reduction in rate with both increased χ and molecular weight may provide an inherent limitation on both the ability to prepare block copolymers by solvent-free melt methods and reactive compatibilization of polymer blends.

Acknowledgment. We thank Bongjin Moon for synthesizing some of the polymers used here. We also thank Thomas R. Hoye and Jianbin Zhang of the University of Minnesota for useful discussions and NSERC Canada, NSF (CTS95 27940), and the NSF-sponsored Center for Interfacial Engineering and IPRIME (Industrial Partnership for Research in Interfacial and Materials Engineering) at the University of Minnesota for supporting this research.

References and Notes

(1) Liu, N. C.; Baker, W. E. *Adv. Polym. Technol.* **1992**, *11*, 249−262.
(2) Lorenzo, M. L.; Frigione, M. *J. Polym. Eng.* **1997**, *17*, 429−459.
(3) Scott, C. E.; Lazo, N. D. B. In *Reactive Polymer Blending*; Baker, W. E., Scott, C. E., Hu, G.-H., Eds.; Hanser: Munich, 2001; pp 114−141.
(4) Martin, P.; Carreau, P. J.; Favis, B. D.; Jerome, R. *J. Rheol.* **2000**, *44*, 569−583.
(5) Lepers, J.-C.; Favis, B. D. *AIChE J.* **1999**, *45*, 887−895.
(6) Scott, C. E.; Macosko, C. W. *Polymer* **1995**, *36*, 461−470.
(7) Orr, C. A. Ph.D. Thesis, University of Minnesota, 1997.
(8) Orr, C. A.; Adedeji, A.; Hirao, A.; Macosko, C. W.; Bates, F. S. *Macromolecules* **1997**, *30*, 1243−1246.
(9) Ibuki, J.; Charoensirisomboon, P.; Chiba, T.; Ougizawa, T.; Inoue, T.; Weber, M.; Koch, E. *Polymer* **1999**, *40*, 647−653.
(10) Charoensirisomboon, P.; Chiba, T.; Solomko, S. I.; Inoue, T.; Weber, M. *Polymer* **1999**, *40*, 6803−6810.
(11) Yin, Z.; Koulic, C.; Pagnoulle, C.; Jerome, R. *Macromolecules* **2001**, *34*, 5132−5139.
(12) Pernot, H.; Baumert, M.; Court, F.; Leibler, L. *Nature Mater.* **2002**, *1*, 54−58.
(13) Guegan, P.; Macosko, C. W.; Ishizone, T.; Hirao, A.; Nakahama, S. *Macromolecules* **1994**, *27*, 4993−4997.
(14) Macosko, C. W.; Jeon, H. K.; Schulze, J. S. In *Encyclopedia of Materials*: *Science and Technology*; Buschow, K. H. J., Cahn, R. W., Flemings, M. C., Ilschner, B., Kramer, E. J., Mahajan, S., Eds.; Elsevier: New York, 2001; Vol. 1, pp 683−688.
(15) Lyu, S.; Cernohous, J. J.; Macosko, C. W.; Bates, F. S. *Macromolecules* **1999**, *32*, 106−110.
(16) Schulze, J. S.; Lodge, T. P.; Macosko, C. W. *Mater. Res. Soc. Symp.* **2000**, *629*, FF2.2.1−6.
(17) Schulze, J. S.; Lodge, T. P.; Macosko, C. W. *Macromolecules*, in preparation.
(18) Yin, Z.; Koulic, C.; Pagnoulle, C.; Jerome, R. *Langmuir* **2003**, *19*, 453−457.
(19) Koriyama, H.; Oyama, H. T.; Ougizawa, T.; Inoue, T.; Weber, M.; Koch, E. *Polymer* **1999**, *40*, 6381−6393.
(20) Jiao, J.; Kramer, E. J.; de Vos, S.; Möller, M.; Koning, C. *Polymer* **1999**, *40*, 3585−3588.
(21) Jiao, J.; Kramer, E. J.; de Vos, S.; Möller, M.; Koning, C. *Macromolecules* **1999**, *32*, 6261−6269.
(22) Moon, B.; Hoye, T. R.; Macosko, C. W. *J. Polym. Sci., Part A*: *Polym. Chem.* **2000**, *38*, 2177−2185.
(23) Schulze, J. S.; Moon, B.; Lodge, T. P.; Macosko, C. W. *Macromolecules* **2001**, *34*, 200−205.
(24) Jones, T. D. Ph.D. Thesis, University of Minnesota, 2000.
(25) Cernohous, J. J.; Macosko, C. W.; Hoye, T. R. *Macromolecules* **1997**, *30*, 5213−5219.
(26) Cernohous, J. J.; Macosko, C. W.; Hoye, T. R. *Macromolecules* **1998**, *31*, 3759−3763.
(27) Maric, M.; Ashurov, N.; Macosko, C. W. *Polym. Eng. Sci.* **2001**, *41*, 631−641.
(28) Maric, M.; Macosko, C. W. *Polym. Eng. Sci.* **2001**, *41*, 118−130.
(29) Anastasiadis, S. H.; Russell, T. P.; Satija, S. K.; Majkrzak, C. F. *J. Chem. Phys.* **1990**, *92*, 5677−5691.
(30) Mallakin, A.; Dixon, D. G.; Greenberg, B. M. *Chemosphere* **2000**, *40*, 1435.
(31) Helfand, E.; Tagami, Y. *J. Polym. Sci., Polym. Lett.* **1971**, *9*, 741−746.
(32) Fetters, L. J.; Lohse, D. J.; Graessley, W. W. *J. Polym. Sci., Part B*: *Polym. Phys.* **1999**, *37*, 1023−1033.
(33) Broseta, D.; Fredrickson, G. H.; Helfand, E.; Leibler, L. *Macromolecules* **1990**, *23*, 132−139.
(34) Russell, T. P.; Anastasiadis, S. H.; Menelle, A.; Felcher, G. P.; Satija, S. K. *Macromolecules* **1991**, *24*, 1575−1582.
(35) Machuga, S. C.; Midje, H. L.; Peanasky, J. S.; Macosko, C. W.; Ranz, W. E. *AIChE J.* **1988**, *34*, 1057−1064.
(36) Green, P. F.; Kramer, E. J. *J. Mater. Res.* **1986**, *1*, 202−204.
(37) Schulze, J. Ph.D. Thesis, University of Minnesota, 2001.

(38) Green, P. F.; Russell, T. P.; Jerome, R.; Granville, M. *Macromolecules* **1988**, *21*, 3266−3273.
(39) Balsara, N. P. In *Physical Properties of Polymers Handbook*; Mark, J. E., Ed.; American Institute of Physics Press: Woodbury, NY, 1996; pp 257−268.
(40) Shefelbine, T. A.; Vigild, M. E.; Matsen, M. W.; Hajduk, D. A.; Hillmyer, M. A.; Cussler, E. L.; Bates, F. S. *J. Am. Chem. Soc.* **1999**, *121*, 8457−8465.

MA0344846